Virology 442 (2013) 12–19

Contents lists available at SciVerse ScienceDirect

Virology

journal homepage: www.elsevier.com/locate/yviro

Small RNA populations for two unrelated viruses exhibit different biases in strand polarity and proximity to terminal sequences in the insect host *Homalodisca vitripennis*

Raja Sekhar Nandety [a], Viacheslav Y. Fofanov [b], Heather Koshinsky [b], Drake C. Stenger [c], Bryce W. Falk [a,*]

[a] Department of Plant Pathology, University of California, Davis, CA 95616, USA
[b] Eureka Genomics, 750 Alfred Nobel Drive, Hercules, CA 94547, USA
[c] United States Department of Agriculture, Agricultural Research Service, Parlier, CA 93648, USA

ARTICLE INFO

Article history:
Received 20 February 2013
Returned to author for revisions
30 March 2013
Accepted 6 April 2013
Available online 1 May 2013

Keywords:
Homalodisca vitripennis reovirus
Homalodisca coagulata virus -1
Glassy-winged sharpshooter
Reoviridae
Dicistroviridae

ABSTRACT

Next generation sequence analyses were used to assess virus-derived small RNA (vsRNA) profiles for *Homalodisca coagulata virus-1* (HoCV-1), family *Dicistroviridae*, and *Homalodisca vitripennis reovirus* (HoVRV), family *Reoviridae*, from virus-infected *H. vitripennis*, the glassy-winged sharpshooter. The vsRNA reads were mapped against the monopartite genome of HoCV-1 and all 12 genome segments of HoVRV, and 21 nt vsRNAs were most common. However, strikingly contrasting patterns for the HoCV-1 and HoVRV genomic RNAs were observed. The majority of HoCV-1 vsRNAs mapped to the genomic positive-strand RNA and, although minor hotspots were observed, vsRNAs mapped across the entire genomic RNA. In contrast, HoVRV vsRNAs mapped to both positive and negative-sense strands for all genome segments, but different genomic segments showed distinct hotspots. The HoVRV vsRNAs were more common for 5′ and 3′ regions of HoVRV regions of all segments. These data suggest that taxonomically different viruses in the same host offer different targets for RNA-antiviral defense.

Introduction

RNA interference (RNAi) is a natural cellular process for regulating gene expression and providing an innate defense mechanism against invading viruses and transposable elements in diverse host types. Small RNAs are hallmarks of RNAi activity but different types of small RNAs originate by distinct biogenesis pathways. Thus, small RNAs are classified into three major groups: small interfering RNAs (siRNAs), microRNAs (miRNAs) and Piwi interacting RNAs (piRNAs) (Ding and Lu, 2011). Among these three groups, siRNAs and miRNAs are primarily 20 to 24 nt in length and are processed by double-stranded RNA (dsRNA)-specific Dicer nucleases while piRNAs (23 to 30 nt) are processed in a Dicer-independent manner (Ding and Lu, 2011). Small RNA duplexes from partial or perfect dsRNA precursors are generated by RNase III family enzymes through sequential endonucleolytic cleavage events (Czech and Hannon, 2011). The resulting products are duplex ~20–24-nt small RNAs consisting of two strands. These small RNAs feature 5′ monophosphates and 2-nt overhangs that have hydroxyl groups at the 3′ termini (Ding and Lu, 2011). Independent of their biogenesis pathway, all three groups of small RNAs associate with Argonaute proteins (AGOs) to mediate RNA cleavage or translational repression (Siomi et al., 2011).

RNAi activity in plants, fungi and nematodes largely depends on amplification of siRNAs by respective cellular RNA-dependent RNA polymerases (RdRPs), which are largely absent in fruit flies, mosquitoes and other insects. However, virus infection of *Rift Valley fever virus* (RVFV) infected mosquito cells resulted in the production of virus-derived small RNAs (vsRNAs) that act as siRNAs (Leger et al., 2013). RNAi activities play significant roles in protecting many organisms, including insects, against infecting viruses (Belles, 2010; Huvenne and Smagghe, 2010). Consequently, this anti-viral RNAi activity may generate a large population of vsRNAs within the virus-infected host. Recent studies using virus-infected cell lines and whole insects have shown that vsRNAs corresponding to both siRNAs and piRNAs may be common (Hess et al., 2011; Leger et al., 2013; Morazzani et al., 2012).

Recent advancements in next generation sequencing (NGS) technologies, such as RNAseq, have led to new opportunities to analyze large populations (tens of millions) of small RNAs (Schuster, 2008; Varshney and May, 2012), including those derived from viral genomes. In virus-infected hosts this has facilitated virus discovery and provided new means to validate and/or characterize virus infections (Gausson and Saleh, 2011; Wu et al., 2010). One recent small RNA study of soybean aphid (*Aphis glycines*) (Liu et al., 2011) resulted in the identification of a novel

* Corresponding author.
E-mail address: bwfalk@ucdavis.edu (B.W. Falk).

0042-6822/$ - see front matter © 2013 Elsevier Inc. All rights reserved.
http://dx.doi.org/10.1016/j.virol.2013.04.005

ssRNA positive-strand virus (*A. glycines virus*, AGV), and two other known aphid viruses (*Aphid lethal paralysis virus*, ALPV; *Rhopalosiphum padi virus,* RhPV). Furthermore, NGS of small RNAs from *Dengue virus*-infected mosquitoes showed differences in quality and quantity of small RNAs over time (Hess et al., 2011; Scott et al., 2010).

The glassy-winged sharpshooter, *Homalodisca vitripennis* (Hemiptera: Cicadellidae), is a xylem-feeding leafhopper and an important pest on a wide range of plants including *Citrus* spp., grapes (*Vitis vinifera*) and almonds (*Prunus dulcis*) (Blua and Morgan, 2003; Redak et al., 2004). *H. vitripennis* also serves as a vector for *Xylella fastidiosa,* the causal agent of Pierce's disease of grapevines and citrus variegated chlorosis disease (Backus et al., 2012). Natural populations of *H. vitripennis* harbor two unrelated viruses: *Homalodisca coagulata virus-1* (HoCV-1) of the family *Dicistroviridae* (Hunnicutt et al., 2006) and *H. vitripennis reovirus* (HoVRV) of the family *Reoviridae* (Stenger et al., 2010; Stenger et al., 2009).

HoCV-1 has a monopartite, positive-sense ssRNA genome (9321 nt, exclusive of the polyadenylated 3′-terminus) encoding two large open reading frames located between nt 420–5807 (ORF1) and 5990–8740 (ORF2) (Hunnicutt et al., 2006). In contrast, the genome of HoVRV is composed of 12 dsRNA segments (Stenger et al., 2009). HoVRV genomic dsRNAs, similar to those of other reoviruses, have conserved segment termini at the 5′-ends (GGCG or GGCA) and 3′-ends (UGAU or CGAU) of the positive sense strand; adjacent imperfect inverted repeats have the potential to base pair (Stenger et al., 2009). Other members of the genus *Phytoreovirus* have host ranges including both plants and insects, but HoVRV is only known to infect *H. vitripennis* (Stenger et al., 2009).

Despite accumulating to high titers, HoCV-1 and HoVRV do not cause obvious disease symptoms in *H. vitripennis*. Indeed, some of our *H. vitripennis* colonies are infected by both viruses, yet such colonies remain robust. These colonies provided an opportunity to investigate patterns of vsRNAs derived from two taxonomically distinct viruses in a single insect host. Here, we used high-throughput small RNA sequencing to map and compare populations of RNAi-induced vsRNAs for HoCV-1 and HoVRV in *H. vitripennis*. Interestingly, vsRNA populations derived from HoCV-1 and HoVRV were distinct from one another with respect to bias in strand polarity and proximity to terminal sequences, suggesting that these two taxonomically unrelated viruses offer different RNAi targets during infection of *H. vitripennis*.

Results

Analysis of small RNAs from HoCV-1 and HoVRV-infected H. vitripennis

Sequencing of adult *H. vitripennis* small RNA libraries yielded 22,151,482 reads (Fig. 1a). Small RNA sequencing reads (43% of the total, ~9.5 million) were mapped to an artificial build of the *H. vitripennis* transcriptome (Nandety and Falk, unpublished). Sequences that matched to redundant rRNA and tRNA sequences were eliminated in subsequent steps to generate the unique datasets. Approximately 18% of the total small RNA reads (4,186,078) were unique to the *H. vitripennis* genome (Fig. 1a). Approximately 57% of the small RNA reads (12,620,344) that did not match the *H. vitripennis* transcriptome, upon further analysis, revealed information on biologically significant associated microbes, including viruses and bacteria.

The majority of small RNA sequences from the *H. vitripennis* sequencing libraries were 19–27 nt in length, with the predominant size class being 21 nt (Fig. 1b). These classes of small RNAs are typical for Dicer (Dcr-2) derived products (Ding and Lu, 2011). The length distributions of the small RNA product classes was seen for *Bombyx mori* (silk worm), *Nilaparvata lugens* (brown plant hopper) (Wei et al., 2009) and for *Dengue virus* (DENV-2) infected mosquito cell lines (Hess et al., 2011). The predominance of 21 nt vsRNAs in *H. vitripennis* and *N. lugens* suggests that small RNA biogenesis pathways in these two leafhoppers are likely conserved.

Identification of small RNAs from H. vitripennis viruses

Adult *H. vitripennis* were used as a source of siRNAs to identify viruses infecting *H. vitripennis*. High quality small RNA contigs ($>$ 100 nt) were used as queries in BLAST searches. The resulting BLAST identities were tabulated using perl scripts that identified major identity viral "hits" to HoCV-1 and HoVRV. Two contigs that matched *Taastrup virus* and a single contig match to *Taura syndrome virus* (TSV) also were identified but due to low abundance, these sequences were not further analyzed. HoCV-1 and HoVRV were widely represented in the BLAST results; vsRNAs completely covered the respective virus genomic RNAs. Each of the contigs that had a proper identity match to the known HoCV-1 and HoVRV genomes is represented as an identifier. Presence of HoCV-1 and HoVRV in the source insects also was validated via RT-PCR as described (Hunnicutt et al., 2006; Stenger et al., 2009).

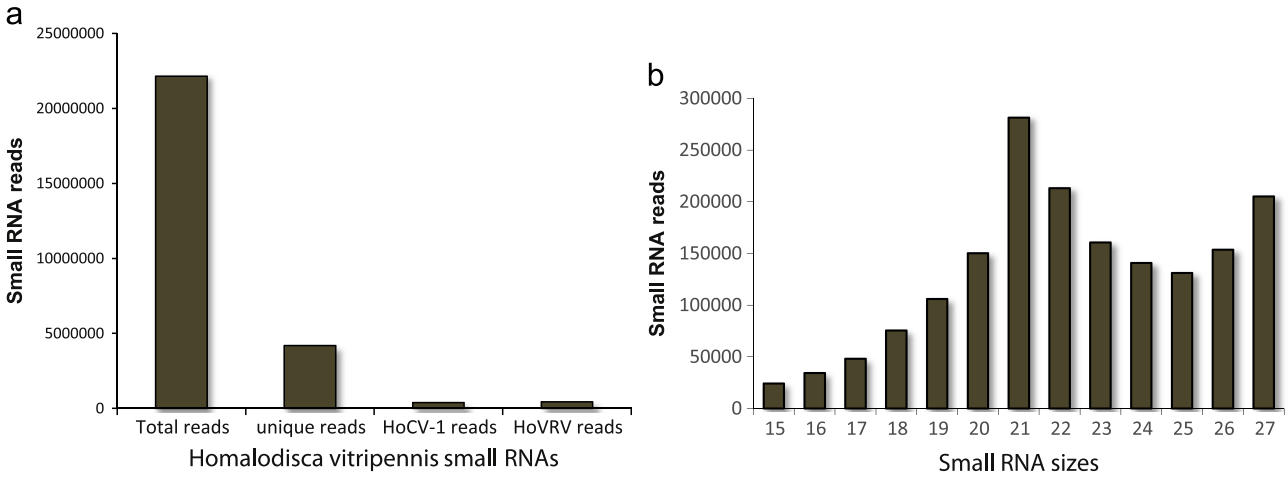

Fig. 1. Small RNA sequencing summary from *Homalodisca vitripennis* adult insects: (a) Graphical summary of total and unique small RNA reads generated from *H. vitripennis* libraries along with the number of small RNA reads that are HoCV-1 and HoVRV specific. (b) Graphical summary of small RNA size classes of the *H. vitripennis* small RNA reads.

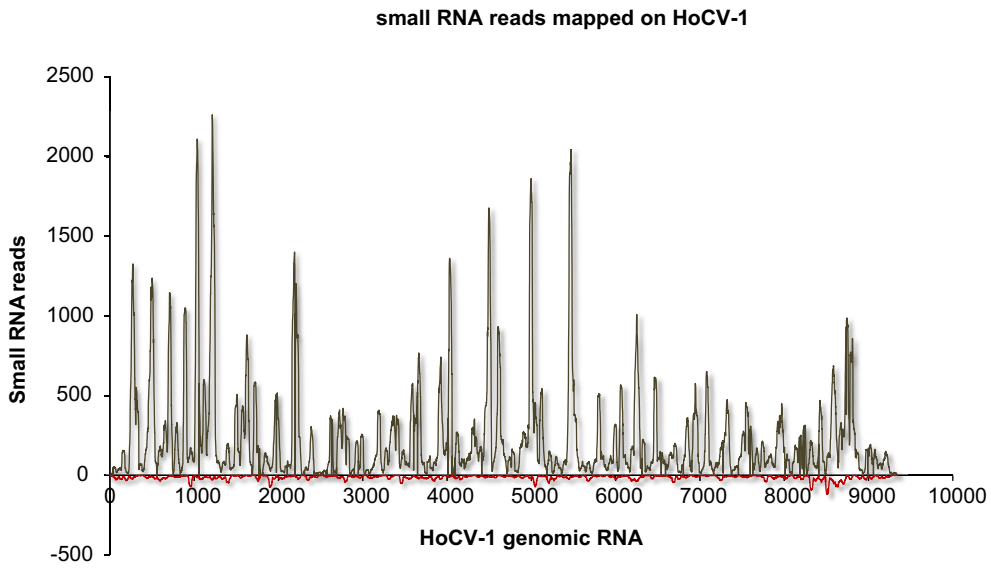

Fig. 2. Mapping summary of vsRNA reads against HoCV-1 genomic RNA. The numbers of vsRNA reads were mapped along the *Y*-axis and the HoCV-1 genomic RNA is represented across the *X*-axis. The grey colored peaks represent the positive-strand small RNAs while the red colored peaks represent the negative-strand small RNAs. (For interpretation of the references to color in this figure legend, the reader is referred to the web version of this article.)

Mapping vsRNAs to the HoCV-1 single-stranded genomic RNA

Nearly 1.7% (386,001) of all small RNA reads corresponded to the HoCV-1 genome. These HoCV-1-specific vsRNAs were aligned into contigs of greater than 100 nt in length (Fig. 1a). The majority of the vsRNA reads mapping to the HoCV-1 genomic RNA were predominantly 21 nt in length. The vast majority (95%, ~350,000) of HoCV-1 vsRNAs were of positive-strand polarity and were not equally distributed across the viral genome (Fig. 2). Small RNA hotspots for HoCV-1 were in the regions encoding the RdRP and the intergenic region between the two ORFs, although subtle continuous distribution was found across the genome. In contrast, the minority of vsRNAs mapping to the HoCV-1 negative strand did not show obvious elevated peaks corresponding to specific regions (Fig. 2).

Small RNA mapping to HoVRV genomic RNAs

Approximately 1.9% (~435,000) of small RNA reads corresponded to the HoVRV genomic RNAs (Fig. 1a), with most being 21 nt in length. Read mapping density and depth at each nucleotide position showed a substantial bias towards the negative-strand of at least four HoVRV segments (segments 1, 2, 8 and 12). Interestingly, these high-density vsRNA clusters all targeted the 3′ terminal regions of the respective negative-sense RNAs (Fig. 3). Similarly, for segments 1, 3, 6, 7, 10 and 11, the 3′ terminal regions of the positive-sense RNAs showed a large cluster of vsRNAs mapping to these respective regions. Segment 1 (2200 to 2400 nt) was the only HoVRV positive sense sequence showing a large, internal cluster of vsRNAs (Fig. 3).

Strand biased nature of the vsRNAs mapping to the genomic RNAs of HoCV-1 and HoVRV

Mapping of vsRNA reads for HoCV-1 and HoVRV showed distinct patterns specific to the RNA strand polarity for each virus. HoCV-1 is a positive-sense ssRNA virus and by far the majority of mapped vsRNAs at each nucleotide position corresponded to the positive-strand (2,209,172) with 18 fold less mapping to the negative-strand (117,858) (Fig. 4a). By contrast, the vsRNAs mapping at each nucleotide position onto HoVRV genomic RNAs were more equally distributed between both strands for most segments. Of the 12 HoVRV dsRNAs, segments 1, 2, 8 and 12 showed more vsRNAs mapping to the negative-strand as compared to the positive-strand (Fig. 4b). Strand bias of total vsRNA fine mapping to segments 2 and 12 was more than 2-fold compared to segments 1 and 8 (Fig. 4b). The remaining segments showed nearly equivalent numbers of vsRNAs mapping to each strand.

Because the data showed clusters of vsRNAs mapping to specific genomic regions/polarities for each virus, quantitative small RNA northern hybridization analysis was used to confirm these data. Two regions of HoVRV segment 1 were examined: vsRNAs of Region 1 (nts 1–200) showed a negative strand bias, whereas vsRNAs of Region 2 (2200–2400 nt) were biased towards the positive strand. Northern hybridization of small RNAs (Fig. 5) confirmed strand biases for Regions 1 and 2. A strong hybridization signal was seen for the negative-sense strand as compared to the positive-sense strand for HoVRV segment 1 Region 1 (Fig. 5, upper panel). In contrast a stronger hybridization signal for positive-sense, compared to negative sense was observed for small RNAs corresponding to HoVRV segment 1 Region 2 (Fig. 5, middle panel).

Potential hotspots for high density of small RNA mapping

Clearly, the above data suggest that there are vsRNA hotspots for the HoCV-1 and HoVRV genomic RNAs. While HoCV-1 shows a strong positive-strand bias with vsRNA distributed across the genomic RNA, HoVRV shows more distinct hot spot regions with some vsRNAs more intensely mapping on the positive-sense strands and some on the negative-sense strands. For the majority of the 12 HoVRV segments, hot spots were present within 100–150 nucleotides of both termini (Fig. 6). It is interesting to note that these hotspots are mostly within untranslated regions (UTRs) (Stenger et al., 2009). Though UTRs only span a few nucleotides of up to 50 bases in either direction, the near imperfect repeats located near segment termini result in the potential panhandle structures of reovirus mRNAs (Stenger et al., 2009) that might account for the unusual terminal distribution of vsRNAs of HoVRV relative to HoCV-1. Among the 12 HoVRV segments, three segments (segments 1, 3 and 12) had regions of vsRNA high density mapping at regions other than termini (Fig. 6). HoVRV segments 1 and 12 show distinct high density vsRNA read mapping on the positive strand between nucleotides 2214 to 2263 and 204 to 272, respectively, while segment 3 exhibits distinctive vsRNA read

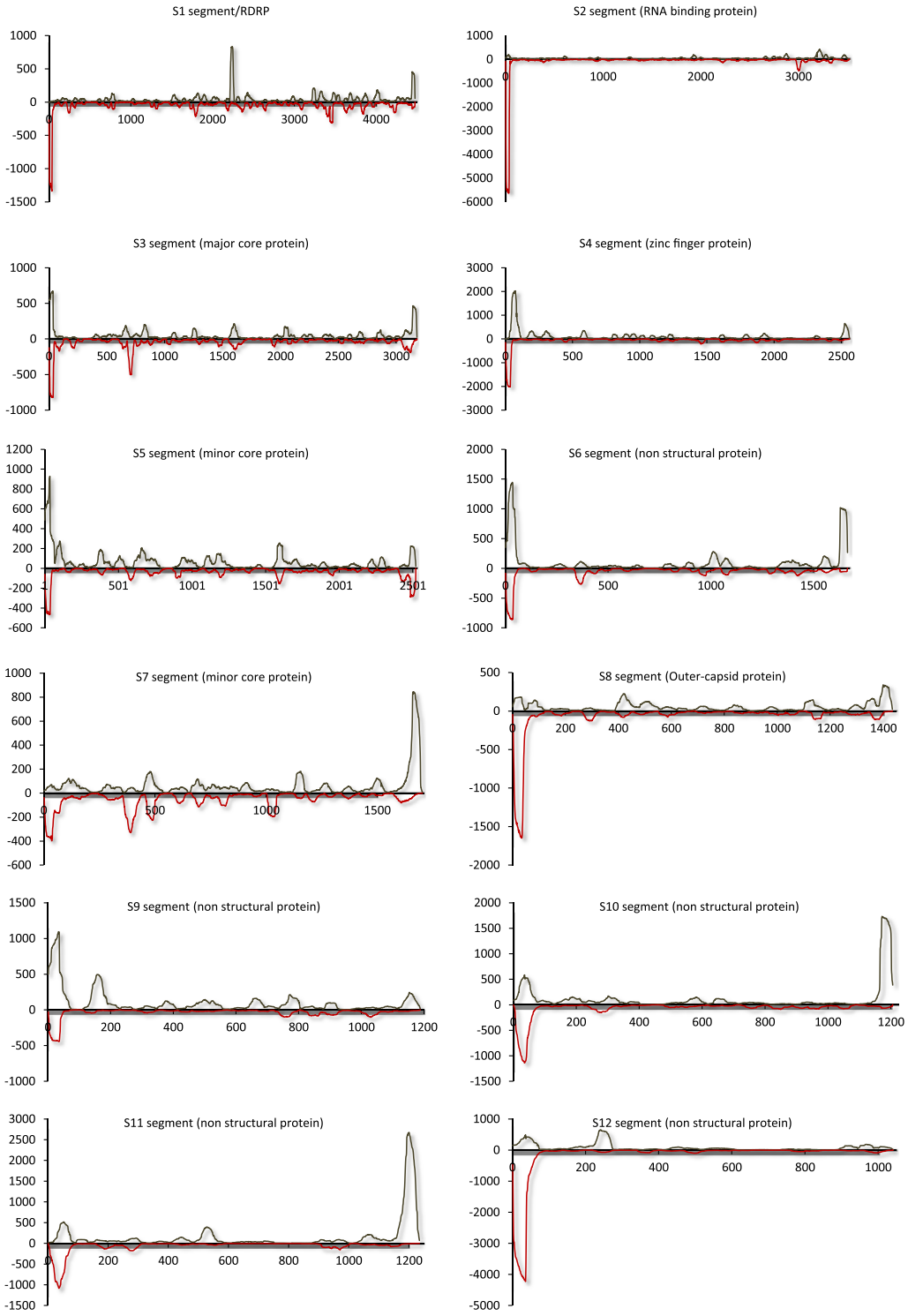

Fig. 3. Mapping summary of vsRNA reads against HoVRV genomic RNAs. The vsRNA reads were mapped along the *Y*-axis and the HoVRV genomic RNAs are represented across the *X*-axis. The grey colored peaks represent the reads on the positive-strand vsRNAs while the red colored peaks represent the reads on the negative-strand vsRNAs. Each panel is for a separate segment S1–S12. (For interpretation of the references to color in this figure legend, the reader is referred to the web version of this article.)

mapping on the negative strand between 681 to 732 nucleotides (Fig. 6).

Discussion

Next generation sequencing approaches offer great tools for virology, including comparison of RNAi and small RNA responses to infection, and discovery of new viruses (Wu et al., 2010). Mapping ratios of small RNAs plotted against viral genomic RNAs (vsRNAs) can reveal a distinct picture of strand bias and polarity, as well as identification of specific regions targeted by the host immune response, as illustrated by the vsRNA populations for HoCV-1 and HoVRV described here. The vsRNA profile was highly skewed towards the positive strand for HoCV-1 (Figs. 2 and 4a) while same was not true for HoVRV genomic RNAs. For HoVRV, the

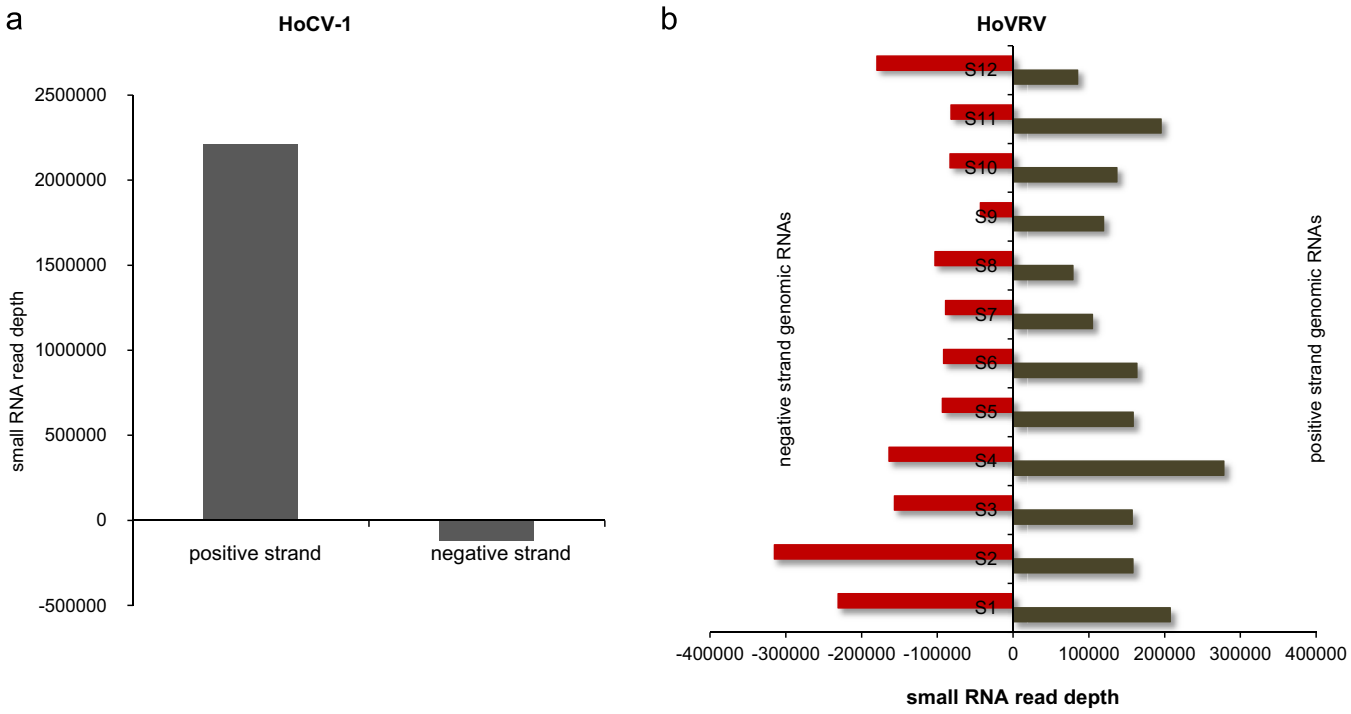

Fig. 4. Small RNA density of *Homalodisca vitripennis* vsRNA reads against the HoCV-1 and HoVRV genomic RNAs. (a) Comparison of total vsRNA read depths on the positive-strand and negative-strand of HoCV-1 genomic RNA. (b) Comparison of total vsRNA read depths and strand ratios on the positive-strand and negative-strand for all HoVRV genomic RNAs.

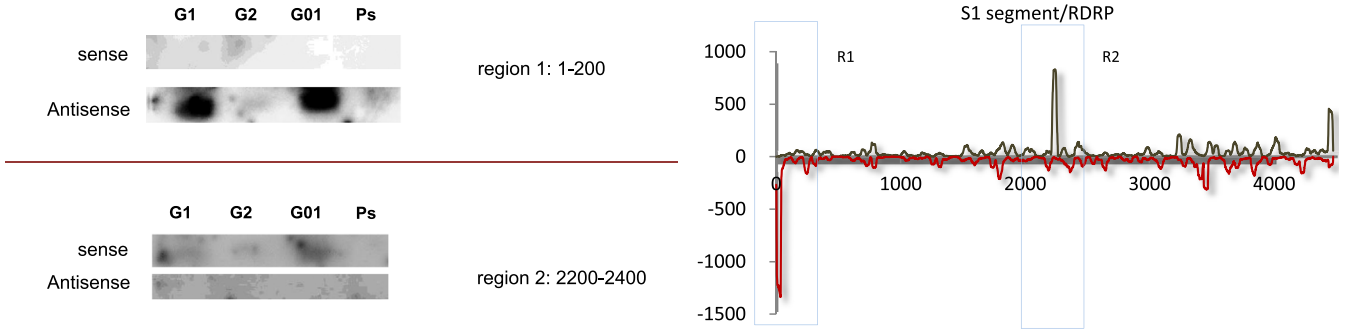

Fig. 5. Quantitative small RNA northern hybridization comparing the strand biased nature of vsRNAs for two different regions of HoVRV segment one RNA. **Upper blot:** Comparison of small RNA hybridization on the positive-strand and negative-strand of the region one (**R1**: 1–200 nt) of the HoVRV segment one. **Lower blot:** Comparison of vsRNA reads on the positive and negative-strand of the region two (**R2:** 2200–2400 nt) of the HoVRV segment one. **Graph:** VsRNA mapping summary of HoVRV segment one genomic RNA with regions one and two marked as blue outlined boxes. **Annotation: G1 and G2:** two different adult *H. vitripennis* samples from our colonies; **G01:** The original insect small RNA sample that was used for sequencing; **Ps:** potato psyllid (*B. cockerelli*) sample used as a negative control. (For interpretation of the references to color in this figure legend, the reader is referred to the web version of this article.)

vsRNAs mapped more often on negative strands compared to positive strands in at least four segments (segments 1, 2, 8 and 12), while vsRNAs for other segments were distributed similarly among both strands (Fig. 3 and Fig. 4b). Recent reports indicate a positive-strand bias of vsRNAs for positive-strand viruses (Donaire et al., 2009; Parameswaran et al., 2010) but, to our knowledge, there are no published data mapping vsRNAs for members of the family *Reoviridae*. One previous report showed the accumulation of vsRNAs to both the strands of *Cryphonectria hypovirus* (CHV1-EP713), a monopartite dsRNA virus species of the genus *Hypovirus*, in a non-random fashion upon infection of the Chestnut blight fungus (*Cryphonectria parasitica*) (Zhang et al., 2008). Because we found differences in polarities and regions targeted for vsRNAs, this suggests that the small RNA libraries analyzed here did not arise from random degradation/shearing of longer viral RNAs. Further, we were able to quantitatively validate vsRNA accumulation for two regions of HoVRV segment 1 with respect to strand polarity and density through the use of quantitative small RNA northern blots on the same sample that was sent for sequencing (Fig. 5).

It is likely that both quality and quantity of vsRNAs are dynamic during the course of infection, development of the insect host from nymph to adult, and also may vary among tissues/organs of the host. Such modulation of small RNAs in different organs has been reported for mice infected with *West Nile virus*, even though the levels of full-length viral RNAs were similar in different organs (Parameswaran et al., 2010). Furthermore, studies with whole mosquitoes and mosquito cell lines show that the types of vsRNAs vary under different conditions (Hess et al., 2011; Scott et al., 2010). Piwi vsRNAs (~26–30 nt) have been shown to be more common in virus infected cell cultures but less common in whole insects (Leger et al., 2013; Wu et al., 2010). In a virus-permissive mosquito cell line, Dicer processing of virus sequence was reported to be disabled (Scott et al., 2010). Our data show that

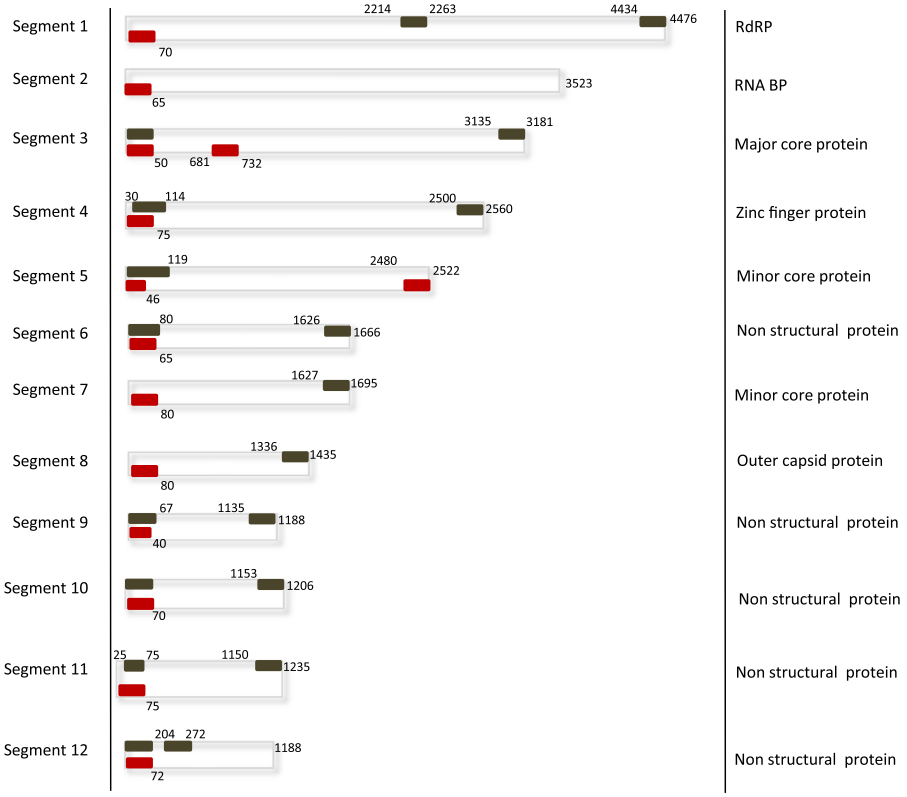

Fig. 6. Structural mapping summary of the vsRNA hotspots on the HoVRV genomic RNAs. The grey boxes represent the regions of vsRNA read depth density on the positive strands of the corresponding segments of HoVRV genomic RNAs. The red boxes represent the regions of vsRNA read depth density on the negative strands of the corresponding segments of the HoVRV genomic RNAs. The numbers adjoining the boxes represent the starting and ending nucleotides where the observed density of vsRNA reads were found. (For interpretation of the references to color in this figure legend, the reader is referred to the web version of this article.)

21 nt vsRNAs were the most abundant forms of vsRNAs for both HoCV-1 and HoVRV.

Viral genomic regions of intense vsRNA density (Fig. 3 and 6), commonly referred to as hotspots (Leger et al., 2013), were observed. The vsRNA hotspots for different regions of both polarities suggest that the seed for production of vsRNAs originates from structures in the individual full-length viral RNAs, and not from a dsRNA replication intermediate. The vsRNA hotspots for HoCV-1 were in the regions encoding the RdRP and the intergenic region between the two ORFs, although subtle continuous distribution was found across the genome. In contrast, for HoVRV the hotspot regions were more distinct and can be readily observed in segments 1 (RdRP), 2 (RNA binding protein), 8 (outer capsid protein) and 12 (Non structural protein). The 3′ regions for most positive- and negative-sense strand HoVRV segments showed hotspots, as did the 5′ regions for a few HoVRV segments. Clearly, the greatest accumulation of vsRNAs was for HoVRV RNA termini (Fig. 6), but some internal hotspots also were seen (e.g. nucleotides 2214 to 2263 for the segment 1 positive strand; see Fig. 6). Strand bias of vsRNAs was observed in Aag2 mosquito cells infected with *Rift Valley fever virus* (RVFV) and it is interesting to note that vsRNAs induced in Aag2 cells after RVFV infection changed during course of infection, with Dicer-2 and Piwi pathways dominating, respectively, at early and late stages of infection (Leger et al., 2013). We examined predictive structures for the HoVRV genomic RNA termini (using RNAfold) in attempts to identify specific or characteristic structural features that might be conserved among the different molecules but found these data to be non-informative. Nonetheless, imperfect repeats located near segment termini are hallmarks of reovirus RNAs that do not occur in the HoCV-1 RNA. Perhaps, the resulting potential panhandle structures of reovirus mRNAs (Chapell et al., 1994; Stenger et al., 2009) act as targets and account for the unusual terminal distribution of vsRNAs of HoVRV relative to HoCV-1. Regardless of the mechanism, the distinct vsRNA mapping patterns observed here with two taxonomically different viruses, HoCV-1 and HoVRV, indicate that different taxa of viruses offer different types of target regions for small RNA biogenesis in the same insect host.

Materials and methods

H. vitripennis maintenance and RNA extraction

Colonies of *H. vitripennis* were maintained at the University of California-Davis Controlled Research Facility (CRF) in cages containing a mixture of plants as described (Rosa et al., 2012). Eight day-old adult insects were collected in three different pools of ~50 insects each. Total RNA samples for each insect pool were extracted using TRIzol reagent (Invitrogen, Carlsbad, CA, USA). The total RNA from each of the insect pools was mixed to reduce any variation and RNA quality was assessed using an Agilent 2100 Bio Analyzer and further processed for small RNA sequencing.

Library preparation and sequence data generation

From each sample, total RNA (2 μg) was used as template to construct single-end indexed llumina small RNA libraries. Samples were processed according to Illumina's TruSeq Small RNA sample preparation guide. Briefly, small RNA was ligated to Illumina's small RNA 3′- and 5′-adaptors, cDNA synthesized by reverse transcription and amplified by PCR with 11 cycles and two size selection gels. Sequencing of the small RNA libraries was performed by the Illumina Genome Analyzer.

Data extraction and analysis

The small RNA sequence reads, after adapter sequence removal, were analyzed using the Velvet (Zerbino and Birney, 2008) and Trinity (Grabherr et al., 2011) assembly programs to identify and generate contigs longer than 100 nucleotides. Assembled contigs were subjected to BLAST analysis (tblastx) (http://blast.ncbi.nlm.nih.gov/Blast.cgi). Perl scripts were written to extract the following relevant data from BLAST output: query sequence name, query sequence length, top match, length of top match, *e*-value for top match, number of matches with *e*-value≤10^{-1} and a list of the next five top matches. Separate scripts were written to parse output from Network BLAST (Altschul et al., 1990).

Mapping small RNAs

Small RNA sequences were mapped onto the indexed HoCV-1 and HoVRV genomic RNAs through the use of Burrows Wheeler Aligner program (BWA) (Li and Durbin, 2009) and Sequence Alignment/Mapping (SAM) programs (Li et al., 2009) along with custom in house Unix scripts. Reference sequences for the two known viruses infecting *H. vitripennis* were: HoCV-1 (NC_008029.1) and HoVRV segment 1 (NC_012535.1), segment 2 (NC_012536.1), segment 3 (NC_012537.1), segment 4 (NC_012538.1), segment 5 (NC_012539.1), segment 6 (NC_012540.1), segment 7 (NC_012541.1), segment 8 (NC_012542.1), segment 9 (NC_012543.1), segment 10 (NC_012544.1), segment 11 (NC_012545.1) and segment 12 (NC_012546.1). The original fastq files for each reference sequence were processed into fasta files using perl scripts; adapter-trimmed read small RNA library data were mapped onto viral genomes using BWA aligner (Li and Durbin, 2009). High quality small RNA reads were processed and assembled into contigs of >100 nt length using the Velvet program (kmer length = 17) (Zerbino and Birney, 2008). The contigs were converted into a fasta format and were analyzed against sequences from the NCBI database (http://blast.ncbi.nlm.nih.gov). Precise mapping of small RNA reads against genomic RNAs was done through the use of BWA aligner (Li and Durbin, 2009) and SAM (Li et al., 2009).

Quantitative small RNA northern hybridization analysis

Quantitative small RNA northern hybridization assays were performed to assay density of small RNAs mapped onto HoVRV segment 1. Briefly, one μg of adult *H. vitripennis* small RNAs were separated on denaturing 8 M urea-15% polyacrylamide gels and transferred to nylon membranes (Amersham Hybond™-NX) as described (Wuriyanghan et al., 2011). One set of probes was designed to target sense and antisense strands of HoVRV segment 1 (1–200 nt), while a second set of probes was designed to target the sense and antisense strands corresponding to nucleotides 2200–2400, also of segment 1. The fragments for each region were PCR amplified from a cDNA clone of HoVRV segment 1 (Stenger et al., 2009) and ligated into pGEM-T-easy in both polarities. Recombinant plasmids containing the corresponding fragment regions in both orientations (sense and antisense) were linearized with Sac I and were used as templates for in vitro transcription with T7 RNA polymerase (Wuriyanghan et al., 2011). Purified ^{32}P-labeled in vitro transcripts for each target were adjusted to 14×10^6 cpm, fragmented to ~300 nt in a solution of 120 mM Na_2CO_3, 80 mM $NaHCO_3$ at 65 °C for 30 min and used for hybridization as described (Wuriyanghan et al., 2011). After washing, blots for each HoVRV segment 1 region were placed in the same cassette and exposed to X-ray film for 36 h at −80 °C. MicroRNA Marker (New England Biolabs; catalog NO. N2102S) was used on the same gel to estimate RNA sizes.

Acknowledgments

This work was supported by grants awarded to Dr. Bryce W. Falk from the USDA-funded University of California Pierce's Disease Research Grants Program. We would like to thank Jessica Nguyen for sequence data generation, Maria Shin for library preparation and sequence data generation and Jingtao Liu for assistance in sequence data analysis. We thank Tera L Pitman for assistance with insect colony maintenance.

References

Altschul, S.F., Gish, W., Miller, W., Myers, E.W., Lipman, D.J., 1990. Basic local alignment search tool. J. Mol. Biol. 215, 403–410.
Backus, E.A., Andrews, K.B., Shugart, H.J., Carl Greve, L., Labavitch, J.M., Alhaddad, H., 2012. Salivary enzymes are injected into xylem by the glassy-winged sharpshooter, a vector of *Xylella fastidiosa*. J. Insect. Physiol. 58, 949–959.
Belles, X., 2010. Beyond Drosophila: RNAi in vivo and functional genomics in insects. Annu. Rev. Entomol. 55, 111–128.
Blua, M.J., Morgan, D.J., 2003. Dispersion of *Homalodisca coagulata* (Hemiptera: Cicadellidae), a vector of *Xylella fastidiosa*, into vineyards in southern California. J. Econ. Entomol. 96, 1369–1374.
Chapell, J.D., Goral, M.I., Rodgers, S.E., dePamphilis, C.W., Dermody, T.S., 1994. Sequence diversity within the reovirus S2 gene: reovirus genes reassort in nature, and their termini are predicted to form a panhandle motif. J. Virol. 68, 750–756.
Czech, B., Hannon, G.J., 2011. Small RNA sorting: matchmaking for Argonautes. Nat. Rev. Genet. 12, 19–31.
Ding, S.W., Lu, R., 2011. Virus-derived siRNAs and piRNAs in immunity and pathogenesis. Curr. Opin. Virol. 1, 533–544.
Donaire, L., Wang, Y., Gonzalez-Ibeas, D., Mayer, K.F., Aranda, M.A., Llave, C., 2009. Deep-sequencing of plant viral small RNAs reveals effective and widespread targeting of viral genomes. Virology 392, 203–214.
Gausson, V., Saleh, M.C., 2011. Viral small RNA cloning and sequencing. Methods Mol. Biol. 721, 107–122.
Grabherr, M.G., Haas, B.J., Yassour, M., Levin, J.Z., Thompson, D.A., Amit, I., Adiconis, X., Fan, L., Raychowdhury, R., Zeng, Q., Chen, Z., Mauceli, E., Hacohen, N., Gnirke, A., Rhind, N., di Palma, F., Birren, B.W., Nusbaum, C., Lindblad-Toh, K., Friedman, N., Regev, A., 2011. Full-length transcriptome assembly from RNA-Seq data without a reference genome. Nat. Biotechnol. 29, 644–652.
Hess, A.M., Prasad, A.N., Ptitsyn, A., Ebel, G.D., Olson, K.E., Barbacioru, C., Monighetti, C., Campbell, C.L., 2011. Small RNA profiling of Dengue virus-mosquito interactions implicates the PIWI RNA pathway in anti-viral defense. BMC Microbiol. 11, 45.
Hunnicutt, L.E., Hunter, W.B., Cave, R.D., Powell, C.A., Mozoruk, J.J., 2006. Genome sequence and molecular characterization of *Homalodisca coagulata virus*-1, a novel virus discovered in the glassy-winged sharpshooter (Hemiptera: Cicadellidae). Virology 350, 67–78.
Huvenne, H., Smagghe, G., 2010. Mechanisms of dsRNA uptake in insects and potential of RNAi for pest control: a review. J. Insect Physiol. 56, 227–235.
Leger, P., Lara, E., Jagla, B., Sismeiro, O., Mansuroglu, Z., Coppee, J.Y., Bonnefoy, E., Bouloy, M., 2013. Dicer-2- and piwi-mediated RNA interference in rift valley Fever virus-infected mosquito cells. J. Virol. 87, 1631–1648.
Li, H., Durbin, R., 2009. Fast and accurate short read alignment with Burrows–Wheeler transform. Bioinformatics 25, 1754–1760.
Li, H., Handsaker, B., Wysoker, A., Fennell, T., Ruan, J., Homer, N., Marth, G., Abecasis, G., Durbin, R., 2009. The sequence alignment/map format and SAMtools. Bioinformatics 25, 2078–2079.
Liu, S., Vijayendran, D., Bonning, B.C., 2011. Next generation sequencing technologies for insect virus discovery. Viruses 3, 1849–1869.
Morazzani, E.M., Wiley, M.R., Murreddu, M.G., Adelman, Z.N., Myles, K.M., 2012. Production of virus-derived ping-pong-dependent piRNA-like small RNAs in the mosquito soma. PLoS Pathog. 8, e1002470.
Parameswaran, P., Sklan, E., Wilkins, C., Burgon, T., Samuel, M.A., Lu, R., Ansel, K.M., Heissmeyer, V., Einav, S., Jackson, W., Doukas, T., Paranjape, S., Polacek, C., dos Santos, F.B., Jalili, R., Babrzadeh, F., Gharizadeh, B., Grimm, D., Kay, M., Koike, S., Sarnow, P., Ronaghi, M., Ding, S.W., Harris, E., Chow, M., Diamond, M.S., Kirkegaard, K., Glenn, J.S., Fire, A.Z., 2010. Six RNA viruses and forty-one hosts: viral small RNAs and modulation of small RNA repertoires in vertebrate and invertebrate systems. PLoS Pathog. 6, e1000764.
Redak, R.A., Purcell, A.H., Lopes, J.R., Blua, M.J., Mizell 3rd, R.F., Andersen, P.C., 2004. The biology of xylem fluid-feeding insect vectors of *Xylella fastidiosa* and their relation to disease epidemiology. Annu. Rev. Entomol. 49, 243–270.
Rosa, C., Kamita, S.G., Falk, B.W., 2012. RNA interference is induced in the glassy winged sharpshooter *Homalodisca vitripennis* by actin dsRNA. Pest Manag. Sci. 68, 995–1002.
Schuster, S.C., 2008. Next-generation sequencing transforms today's biology. Nat. Methods 5, 16–18.
Scott, J.C., Brackney, D.E., Campbell, C.L., Bondu-Hawkins, V., Hjelle, B., Ebel, G.D., Olson, K.E., Blair, C.D., 2010. Comparison of dengue virus type 2-specific small RNAs from RNA interference-competent and -incompetent mosquito cells. PLoS Negl.Trop. Dis. 4, e848.

Siomi, M.C., Sato, K., Pezic, D., Aravin, A.A., 2011. PIWI-interacting small RNAs: the vanguard of genome defence. Nat. Rev. Mol. Cell Biol. 12, 246–258.
Stenger, D.C., Sisterson, M.S., French, R., 2010. Population genetics of *Homalodisca vitripennis* reovirus validates timing and limited introduction to California of its invasive insect host, the glassy-winged sharpshooter. Virology 407, 53–59.
Stenger, D.C., Sisterson, M.S., Krugner, R., Backus, E.A., Hunter, W.B., 2009. A new Phytoreovirus infecting the glassy-winged sharpshooter (*Homalodisca vitripennis*). Virology 386, 469–477.
Varshney, R.K., May, G.D., 2012. Next-generation sequencing technologies: opportunities and obligations in plant genomics. Brief. Funct. Genomics 11, 1–2.
Wei, Y., Chen, S., Yang, P., Ma, Z., Kang, L., 2009. Characterization and comparative profiling of the small RNA transcriptomes in two phases of locust. Genome Biol. 10, R6.
Wu, Q., Luo, Y., Lu, R., Lau, N., Lai, E.C., Li, W.X., Ding, S.W., 2010. Virus discovery by deep sequencing and assembly of virus-derived small silencing RNAs. PNAS 107, 1606–1611.
Wuriyanghan, H., Rosa, C., Falk, B.W., 2011. Oral delivery of double-stranded RNAs and siRNAs induces RNAi effects in the potato/tomato psyllid, *Bactericerca cockerelli*. PLoS One 6, e27736.
Zerbino, D.R., Birney, E., 2008. Velvet: algorithms for de novo short read assembly using de Bruijn graphs. Genome Res. 18, 821–829.
Zhang, X., Segers, G.C., Sun, Q., Deng, F., Nuss, D.L., 2008. Characterization of hypovirus-derived small RNAs generated in the chestnut blight fungus by an inducible DCL-2-dependent pathway. J. Virol. 82, 2613–2619.